Circuits, Systems, and Signal Processing (2021) 40:2895–2925
https://doi.org/10.1007/s00034-020-01602-8

Design of Optimal FIR Filters Using Integrated Optimization Technique

Teena Mittal[1]

Received: 20 February 2020 / Revised: 10 November 2020 / Accepted: 13 November 2020 /
Published online: 27 November 2020

Abstract
The aim of the research work is to optimally design a finite impulse response (FIR) filter. For this purpose, an integrated optimization technique has been proposed. The proposed optimization technique integrates the Moth flame optimization (MFO) technique and Powell's pattern search (PPS) technique in a coherent manner to maintain a fine balance between exploration and exploitation capabilities of the search technique. During the search process, the best performing MFO particle is transferred to the PPS method to avoid any possible stagnation. Initially, the proposed optimization technique has been tested on five standard test functions and then it is applied to design optimal FIR low-pass, high-pass, band-pass and band-stop filters. The performance of the proposed optimization technique is compared with other state of art optimization techniques and also with the results reported in the literature. The proposed optimization technique yields high-quality solution with minimal computational efforts. Further, student t test is applied to test the statistical performance of optimization technique and found satisfactory.

Keywords FIR filter design · Integrated optimization technique · Moth flame optimization · Powell's pattern search

1 Introduction

In the current scenario, the signal has a significant role in the digital signal processing (DSP) systems. Most of the signals have inherent noise and also get distorted with external noise; hence there is a need of digital filters to achieve the desired spectral characteristics. The basic building blocks of DSP systems are digital filters. Depending on the duration of the impulse response, digital filters are categorized into finite impulse

✉ Teena Mittal
tnarang28@gmail.com

[1] Department of Electronics and Communication Engineering, Thapar Institute of Engineering and Technology, Patiala, Punjab 147004, India

response (FIR) filter and infinite impulse response (IIR) filter [15]. The implementation of FIR filters uses non-recursive structures and having many desired advantages. The coefficients of linear phase FIR filter are symmetrically located around the central coefficient, and these filters are simple to design than IIR filters. The researchers have applied conventional methods to design digital filters such as window method and frequency sampling method. Various types of window function, i.e. Kaiser, Blackmann, Hanning, Hamming have been used as per filter specifications. In windowing method, for an ideal filter, the infinite length impulse response is approximated into a window of finite length to accomplish the real response [15, 25, 26]. However, due to this approximation, it does not permit the precise control of cut-off frequencies and the transition width. For the design of FIR filter, Parks and McCellan [25] have suggested a well-known method named as 'PM algorithm', which is based on Chebyshev approximation method. In PM method, the weighting function is applied to determine the relative values of the amplitude error in the frequency bands and not by the deviations themselves. Hence, the PM method requires many iterative cycles to design the digital filter [26]. McClellan et al. [17] have reported improved results as compared to the results obtained by PM algorithm. These classical methods are single-point search methods and solution struck at a local optimal point for multi-modal optimization problems. Further, these methods are not suited for optimization problems having discontinuous and non-differentiable objective function.

In order to overcome these drawbacks of conventional techniques, the researchers have proposed population-based search techniques. For the design of FIR filters, a number of population-based search techniques have been implemented in the recent years. Karaboga and Cetinkaya [10] have applied differential evolution technique for the design of digital FIR filter. The fuzzy adaptive simulated annealing technique has been implemented to design FIR filters [24]. Kar et al. [8] have proposed craziness-based PSO technique and employed for FIR stop-band filter. Saha et al. [28] have applied cat swarm optimization (CSO) technique to determine the optimal coefficients of FIR filters. Aggarwal et al. [2] have applied the L_1-norm based real-coded genetic algorithm to search optimal coefficients of high-pass FIR filter. In another attempt, few evolutionary and swarm-based optimization techniques have also been applied for the design of digital FIR filters by Aggarwal et al. [1]. For the design of the optimal FIR filter and multi-band filters, the adaptive cuckoo search algorithm [30] and improved cuckoo search PSO technique [5] have also been applied, respectively.

The digital filters encounter the problem of time delays. Hence, researchers give much attention to the stability problem of digital filters. The Markovian jump systems are an effective tool for the design of filters. Researchers are continuously working to deal with issues related to Markovian jump system. Recently, Xia et al. [36] have addressed the problem of mixed passivity and H_∞ filter design for a class of Markovian jump delay systems with nonlinear perturbation under quantization and event-triggered scheme. In another attempt, the problem of extended dissipativity analysis for digital filters which simultaneously consists time delay and Markovian jumping parameters have been addressed [37]. Xia et al. [35] have extended the work to deal with the problem of filter design for discrete-time neural networks subject to Markovian jumping parameters and time-varying delay.

The population-based search techniques have been classified into different categories, namely evolutionary techniques, physics-based techniques, swarm-based techniques etc. Recently, Mirjalili [19] has suggested a swarm-based algorithm, Moth-flame optimization, which is a nature-inspired algorithm based on the navigation mechanism of Moths in transverse orientation. The MFO technique has been used to resolve various practical optimization problems, i.e. optical network unit placement in fibre-wireless access network [31], optimal reactive power dispatch [18, 21], thresholding image segmentation [3], unit commitment problem [27], and circular antenna array synthesis [4].

The MFO technique is inspired by Moths navigation method in the night. The Moths fly by making a certain angle corresponding to the moon. By using this process, they travel for long distances in a straight line. Nevertheless, these Moths can simply confuse due to artificial lights. The researchers have proposed various modifications in the MFO technique or integrated with other optimization techniques for better performance. Li et al. [13] have proposed Lévy-flight strategy-based MFO (LMFO) and tested on constrained and unconstrained benchmark functions successfully. Elsakaan et al. [6] have proposed enhanced MFO algorithm which combines the merits of the MFO and Lévy flight search. The enhanced MFO has been applied to solve economic dispatch problem with emissions. Recently, a Moth search algorithm [14, 33] has been proposed, which is inspired by the phototaxis and Lévy flights of the Moths. They have successfully tested the proposed algorithm on benchmark problems. Wang et al. [34] have proposed chaos theory to exploit MFO's potential and to enhance its performance. They have applied proposed technique for parameter optimization of kernel extreme learning machine and feature selection. Khalilpourazari and Khalilpourazary [12] have proposed an integration of water cycle optimization algorithm and MFO algorithm to solve the constraint optimization problems. Zhang et al. [39] have proposed an evolutionary algorithm by exploiting the spiral search behaviour of Moths and also incorporates search actions of fireflies to explore the search space. The proposed algorithm has been applied for intelligent facial emotion recognition. Xu et al. [38] have integrated Gaussian mutation, Cauchy mutation, Levy mutation and combination of these with MFO technique and tested on benchmark functions. They have concluded that the integrate technique is able to search better quality results as compared to other population-based techniques. Despite of the various advantages of global search techniques, the exploitation capability of these algorithms is inferior as compared to local search techniques [7]. However, local search techniques are computationally expensive and can easily trap into local optimal solution due to single-point search. The Powell's pattern search as a potential local search technique has been applied by researchers and its performance has been found very promising [22, 23].

In this work, an integrated optimization technique has been proposed to maintain a fine tuning between exploration and exploitation capability of the search algorithm. In the proposed technique, the search process initiates with MFO technique and a move to the PPS method by an adaptive mechanism and this process continues till the termination criteria. In the light of these observations, the main contributions of the research work are summarized as:

- An integrated optimization technique has been aimed to incorporate the positive traits of global and local search techniques.
- The MFO and PPS techniques have been undertaken as a global and local search technique, respectively. In the proposed technique, the best performing MFO particle transferred to PPS technique in an adaptive manner for further improvement.
- The proposed optimization technique has been implemented to solve standard benchmark functions and for designing of optimal FIR filters.

The paper is structured into five sections. The design formulation of FIR filter is given in Sect. 2. In Sect. 3, the proposed optimization technique has been presented. In Sect. 4, results and discussion are discussed and finally, Sect. 5 outlines the conclusions.

2 FIR Filter Design Formulation

In this section, the mathematical model of various types of FIR filters, i.e. low pass, high pass, band pass and band stop has been presented. The impulse response of FIR filter in terms of Z-Transform is given as:

$$H(z) = h(0) + h(1)z^{-1} + h(2)z^{-2} + \cdots, h(N)z^{-N} \tag{1}$$

where $h(0)$, $h(1)$, …, $h(n)$ represents the impulse response of FIR filter; hence Nth order filter requires a $N + 1$ number of coefficients.

Equation (1) is represented as:

$$H(z) = \sum_{n=0}^{N} h(n)z^{-N} \tag{2}$$

The frequency response of the FIR filter is given as:

$$H(\omega_k) = \sum_{n=0}^{N} h(n)e^{-j\omega_k n} \tag{3}$$

where $H(\omega_k)$ represents Fourier transform complex vector; The frequency is sampled in the range of $[0, \pi]$ with N sample points and $\omega_k = (2\pi/N)$.

The magnitude response of the ideal filter is given as:

$$H_i(\omega) = \begin{cases} \begin{cases} 1 & 0 \le \omega \le \omega_c \\ 0 & \text{otherwise} \end{cases}; & \text{LP} \\ \begin{cases} 0 & 0 \le \omega \le \omega_c \\ 1 & \text{otherwise} \end{cases}; & \text{HP} \\ \begin{cases} 1 & \omega_{\text{cl}} \le \omega \le \omega_{\text{ch}} \\ 0 & \text{otherwise} \end{cases}; & \text{BP} \\ \begin{cases} 0 & \omega_{\text{cl}} \le \omega \le \omega_{\text{ch}} \\ 1 & \text{otherwise} \end{cases}; & \text{BS} \end{cases} \tag{4}$$

where $H_i(\omega)$ represents the ideal magnitude response; ω_{cl} and ω_{ch} represent the lower and upper cut-off frequency, respectively, of the BP and BS filters.

In this work, Type-I linear phase FIR filter has been designed using optimization techniques. The FIR filter has a symmetrical impulse response, hence the number of decision variables to be searched is halved and the remaining half-coefficients are flipped to determine the complete impulse response. To design the FIR filter with quality attributes, i.e. higher stop-band attenuation, lower stop-band and pass-band ripples, control on the transition width, and the suitable objective function, needs to be chosen. Parks and McClellan [25] have been proposed one of the most extensively used error function and is given as:

$$E(\omega) = G(\omega)\left[H_d\left(e^{j\omega}\right) - H_i\left(e^{j\omega}\right)\right] \tag{5}$$

where $H_i(e^{j\omega})$, $H_d(e^{j\omega})$ represent the ideal and desired magnitude response, respectively; $G(\omega)$ represents the weighting factor to provide approximate errors in different frequency ranges.

Saha et al. [28] have discussed various error functions and recommended a novel error function as an objective function, which is given as:

$$E(\omega) = \sum \text{abs}\left[\text{abs}\left|(H_d(\omega) - 1) - \delta_p\right| + \sum \text{abs}(|H_d(\omega) - 0| - \delta_s)\right] \tag{6}$$

where δ_p represent the pass-band ripples and δ_s represent the stop-band ripples.

Equation (6) considers absolute errors for entire frequency range. The first term represents a frequency range of pass-band and second term incorporates the stop-band frequency range. Higher stop-band attenuation and lesser stop-band ripples can be provided by minimizing the total error between the ideal magnitude response and the desired magnitude response over the entire frequency range. Further, the transition width may also get reduces.

3 Overview of Optimization Techniques

In this work, FIR filter design problem is solved by applying PSO, chaotic DE, artificial bee colony, GWO, MFO and proposed optimization technique to prove the merit of the proposed optimization technique. In this section, a brief discussion of the applied algorithms is given and the detail description of proposed technique has been discussed.

3.1 Particle Swarm Optimization

In particle swarm optimization technique, the search procedure is inspired by bird flocking or fish swarm behaviour [11]. All through the exploration, each particle updates its position through the guidance of global best position and local best position. For a d dimension search space, the velocity vector and position vector of ith

particle are represented by: $V_i = \left(v_i^1, v_i^2, \ldots, v_i^d\right)$ and $P_i = \left(p_i^1, p_i^2, \ldots, p_i^d\right)$. The particle velocity and position are updated according to Eqs. (7) and (8).

$$v_i^j \leftarrow w v_i^j + c_1 \times \text{rand}() \times \left(pl_i^j - x_i^j\right) + c_2 \times \text{rand}() \times \left(pg^j - x_i^j\right) \quad (i \in NP; j \in d) \tag{7}$$

$$w = w^{\max} - \frac{\left(w^{\max} - w^{\min}\right) \times \text{it}}{\text{IT}} \tag{8}$$

$$x_i^j \leftarrow x_i^j + v_i^j \quad (i \in NP; j \in d) \tag{9}$$

where x_i^j, v_i^j represent jth dimension position and velocity, respectively, for ith particle; pl_i^j is jth dimension local best position for ith particle; pg^j is jth dimension global best position; NP is number of particles; c_1, c_2 are acceleration coefficients; $w_{\max}$ is the maximum inertia weight and $\text{w}_{\min}$ is the minimum inertia weight; *rand*() represents the random number, which is uniformly distributed over the range [0,1]. For PSO technique, acceleration coefficients c_1, c_2 have been set to 1.5 and 2.5, respectively. The values of maximum inertia weight and minimum inertia weight $w^{\max}$, $w^{\min}$ have been set to 0.95 and 0.35, respectively.

3.2 Chaotic Differential Evolution

In DE algorithm, the search evolves by mutation, recombination and selection operators to achieve an optimal solution. The mutation operator adds a vector difference between two arbitrarily chosen population vectors to the parent population vector and is given as [29]:

$$y_i^j \leftarrow x_{i,r1}^j + f_m\left(x_{i,r2}^j - x_{i,r3}^j\right) \quad (i \in NP; j \in d) \tag{10}$$

where $r1$, $r2$, $r3$ are mutually different integers and these integers should also be different from the population index i; f_m represents the mutation scale factor.

The search approach of DE and chaotic optimization is contradictory in nature. The DE technique is based on natural evolution and chaotic sequences display an unpredictable, irregular behaviour. This characteristic of chaotic sequences is useful to improve the search capability of DE algorithm. Hence, in this work, chaotic sequence based on logistic map approach has been applied to modify the mutation scale factor as:

$$y_i^j \leftarrow x_{i,r1}^j + f_1(t)\left(x_{i,r2}^j - x_{i,r3}^j\right) \quad (i \in NP; j \in d) \tag{11}$$

$$f_1(t) \leftarrow \mu \times f_1(t-1) \times [1 - f_1(t-1)] \quad (i \in NP; j \in d) \tag{12}$$

$$f_1(t) \in [0, 1]$$

where t represents the iteration count, $f_1(t)$ represents the mutation scale factor, which is based on logistic map, and μ is a control parameter; $f_1(t) \notin \{0, 0.25.0.50, 0.75, 1\}$.

Following the mutation operation, crossover process is employed to produce a trial vector z_i^j between targeted vector x_i^j and intermediate vector y_i^j as:

$$z_i^j = \begin{cases} x_i^j & \text{rand}()_j > C_R \\ y_i^j & \text{otherwise} \end{cases} \quad (i \in \text{NP}; j \in d) \tag{13}$$

where C_R represents a crossover probability factor from the range [0,1].

After the crossover operation, a greedy selection pattern is applied to select the better individual as:

$$x_i = \begin{cases} z_i & \text{obj}(z_i) < \text{obj}(x_i) \\ x_i & \text{otherwise} \end{cases} \quad (i \in \text{NP}) \tag{14}$$

where obj represents the objective function.

The Chaotic DE algorithm parameters, mutation scale factor f_m is set to 0.5 and the control parameter μ is set to 4.

The whole process continues till termination condition is met.

3.3 Artificial Bee Colony

In artificial bee colony algorithm, the bee population is divided into employed bees, onlooker bees and scout bees. The initial population x_{ij} is evaluated based on nectar amount and employed bees produce new solutions v_{ij} and given as [9]:

$$v_{ij} = x_{ij} + \tau_{ij}(x_{ij} - x_{kj}) \quad (i \in \text{EB}; j \in d; k \in \text{EB}; i \neq k) \tag{15}$$

where τ_{ij} represents a random number between $[-1, 1]$; k individual is randomly selected and should be different from i; EB is the number of employed bees.

The new population has been evaluated and to update the solution, the greedy selection process is used. Based on the objective function evaluation, the probability has been computed as:

$$p_i = \frac{\text{obj}_i}{\sum_{l=1}^{\text{EB}} \text{obj}_l} \tag{16}$$

where obj_i represents the ith candidate objective function value.

The onlookers produce the new solution v_{ij} from the current solution, which is selected based on probability value. The greedy selection process is implemented between current onlooker and new onlooker to update the solution. During the search process, if the nectar value is abandoned for a predetermined number of cycles, then the food source i is replaced with a new food source by the scouts and is given as:

$$x_{ij} = x_j^{\min} + \text{rand}() \times \left(x_j^{\max} - x_j^{\min}\right) \quad (j \in d) \tag{17}$$

The whole procedure is repeated till the satisfaction of termination criteria.

3.4 Grey Wolf Optimization Technique

The grey wolves come under the category of top predators, who like to live and hunt in a group. They follow a very unique and strict social ruling hierarchy. The first best solution is known as alpha (α). Consequently, the second and third best solutions are considered as beta (β) and delta (δ), respectively, and all the remaining solutions are presumed as omega (ω). The α, β and δ surely participate in the hunt process and ω may follow them. The grey wolves follow the few steps as follows [20]:

(i) (i) Tracking and chasing the prey: Grey wolves surround the prey during hunting. The encircling behaviour by grey wolves is mathematically modelled as:

$$Z = |B \times X_P(\text{it}) - X_{\text{GW}}(\text{it})| \tag{18}$$

$$X_{\text{GW}}(\text{it}+1) = X_P(\text{it}) - A \times Z \tag{19}$$

The coefficient vectors$A$ and B are reckoned as:

$$A = 2 \times z \times R_1 - z \tag{20}$$

$$B = 2 \times R_2 \tag{21}$$

$$z = 2 - \frac{2 \times \text{it}}{\text{IT}_{\max}} (\text{it} \in \text{IT}_{\max}) \tag{22}$$

(ii) Hunting of prey: The alpha as a leader guides the hunting process and it is followed by beta and delta. The remaining wolves update their positions with respect to the leader (alpha), beta and delta. The mathematical formulation of the hunting process and updating the positions of grey wolves are expressed as:

$$Z_\alpha = |B_1 \times X_\alpha(\text{it}) - X_{\text{GW}}(\text{it})| \tag{23a}$$

$$X_1(\text{it}) = X_\alpha(\text{it}) - A_1 \times Z_\alpha \tag{23b}$$

$$Z_\beta = \left|B_2 \times X_\beta(\text{it}) - X_{\text{GW}}(\text{it})\right| \tag{24a}$$

$$X_2(\text{it}) = X_\beta(\text{it}) - A_2 \times Z_\beta \tag{24b}$$

$$Z_\delta = |B_3 \times X_\delta(\text{it}) - X_{\text{GW}}(\text{it})| \tag{25a}$$

$$X_3(\text{it}) = X_\delta(\text{it}) - A_3 \times Z_\delta \tag{25b}$$

where X_α, X_β and X_δ are the positions of the three best representatives, i.e. alpha, beta and delta, respectively; X_1, X_2 and X_3 are the prey positions with respect

to alpha, beta and delta. The position of the grey wolves is updated by using the average position of alpha, beta and delta and is given as:

$$X_{\mathrm{GW}}(\mathrm{it}+1) = \frac{X_1(\mathrm{it}) + X_2(\mathrm{it}) + X_3(\mathrm{it})}{3} \tag{26}$$

(iii) Conducting attack: Grey wolves finish their hunt when quarry stops. As the wolves approach the prey, the value of z gradually goes towards zero and prey is supposed to be attacked by grey wolves.

3.5 Moth Flame Optimization

Mirjalili [19] has proposed a MFO technique, which is based on navigation mechanism of Moths. The Moth insects fly at night by keeping a certain angle with the moon. This particular mechanism is called the transverse orientation. The transverse orientation is very useful for the Moths to travel long distances; however, Moths gets distracted by human-made artificial lights. They seek to hold the fixed angle to the light source, due to which they may eventually converge to the artificial light source. The mathematical model of MFO technique restrains all the properties. The mathematical model of an optimizer has been discussed as under:

The set of Moths represent the candidate solutions. Initially, each Moth position is randomly generated within inside the limited boundary. For each Moth, the objective function has been evaluated. The flames represent the best position of Moths at present iteration. The Moth explores around the flame and position is updated accordingly. In MFO algorithm, the logarithmic spiral mechanism has been utilized to update the status of each Moth corresponding to a flame and is given as:

$$M_i = D_i \times e^{\mathrm{bt}} \times \cos(2\pi\, t) + F_j \quad (i \in \mathrm{NP};\, j \in \mathrm{NP}) \tag{27}$$

where M_i represents the ith Moth; F_j represents the jth flame; D_i gives the distance of ith Moth from jth flame; b defines the shape of a spiral; t is a random number between $[-1, 1]$; the value of $t = -1$ and $t = +1$ represent the closest and farthest positions to the flame, respectively, for the logarithmic spiral; NP represent the number of Moths; The random number r generates in the range of $[r,1]$, where r linearly decreases from -1 to -2 with iteration [13].

It is evident from Eq. (27), each Moth is associated with a flame and updates its own position corresponding to a particular flame. On the basis of objective function value, the flames are sorted and the first Moth updates its position using the best flame and last Moth updates the position using the worst flame in the list. The exploitation capability of the algorithm can be improved by decreasing the number of flames adaptively with iterations. The adaptive mechanism is given as:

$$\mathrm{Nf} = \mathrm{round}\left[\left(\mathrm{Nf}^{\max} - \mathrm{it}\right) \times \frac{(\mathrm{Nf}^{\max} - 1)}{\mathrm{IT}}\right] \tag{28}$$

where Nf represents the number of flames; $\mathrm{Nf}^{\max}$ represents the maximum number of flames; it signifies the current iteration; IT signifies the maximum number of iterations.

3.6 Powell's Conjugate Direction Method

The Powell's conjugate direction method is proposed to search the optimal solution [32]. The Powell's method does not require derivative information of function; hence it can be applied to non-differentiable and discontinuous function. For d dimension decision variable, *i.e.*, $X = (x_1, x_2, \ldots, x_d)$, the d search vectors (say $\{s_1, s_2, \ldots, s_d\}$) are generated as:

$$s_j^k = \begin{cases} 1 & j = k \\ 0 & \text{else} \end{cases} \quad (j \in d; k \in d) \tag{29}$$

Each decision variable is modified along with respective search direction and is given as:

$$x_j \leftarrow x_j + \varsigma_j s_j^k \quad (j \in d; k \in d) \tag{30}$$

where ς_j represents the step length for jth dimension and it is randomly generated within the bounds.

In order to update each dimension of decision variable, the greedy selection process has been applied. The updated decision variable is represented as: $X' = (x_1', x_2', \ldots, x_d')$. For the succeeding cycle of optimization, the pattern search direction is computed as: $Z_j(j = 1, 2, \ldots, d) = (x_1 - x_1', x_2 - x_2', \ldots, x_d - x_d')$ and each pattern search direction replaces its corresponding direct search direction. The up-gradation process is repeated with pattern search direction. The search process continues till all the direct search directions discarded.

3.7 Proposed Optimization Technique

In the proposed technique, the best solution obtained by the MFO algorithm (MFO leader) is exploited by PPS technique in a phased manner. The detail explanation of proposed technique is given as:

Step 1: Read the input data and algorithm parameters.
Step 2: Randomly initialize the decision variables as moth positions within the specified limits.
Step 3: Iteration start; it = 1.
Step 4: The objective function (Eq. (6)) is evaluated for each moth position.
Step 5: The moth position is updated (Eq. (27)) with respect to a particular flame.
Step 6: The number of flames decreases as given by Eq. (28).
Step 7: Check the performance of MFO leader for a certain life span (LS) as:

$$\mathrm{IF}\{F(\mathrm{it}) - F(\mathrm{it} + \mathrm{LS}) < \alpha \times F(\mathrm{it})\}$$

Table 1 Benchmark functions for D dimension

S. No	Function	Equation	Search range	Optimum
F_1	Ackley	$f_1(x) = -20\exp\left(-0.2\sqrt{D^{-1}\sum_{i=1}^{D} x_i^2}\right) - \exp\left(D^{-1}\sum_{i=1}^{D}\cos 2\pi x_i\right) + 20 + e$	$[-32, 32]^D$	(0,…,0)
F_2	Griewank	$f_2 = \sum_{i=1}^{D} \frac{x_i^2}{4000} - \prod_{i=1}^{D}\cos\left(\frac{x_i}{\sqrt{i}}\right) + 1$	$[-600, 600]^D$	(0,…,0)
F_3	Rastrigin	$f_3(x) = \sum_{i=1}^{D}\left[x_i^2 - 10\cos(2\pi x_i + 10)\right]$	$[-5.12, 5.12]^D$	(0,…,0)
F_4	Schwefel 2.22	$f_4(x) = \sum_{i=1}^{D}\lvert x_i\rvert + \prod_{i=1}^{D}\lvert x_i\rvert$	$[-10, 10]^D$	(0,…,0)
F_5	Schwefel 2.26	$f_5(x) = 418.98288727243369 \times D - \sum_{i=1}^{D} -x_i \sin\left(\sqrt{\lvert x_i\rvert}\right)$	$[-500, 500]^D$	(420.96, …, 420.96)

$D = 30$

Table 2 The best solutions of Benchmark functions

Function	PSO	Chaotic DE	ABC	GWO	MFO	Proposed technique
F_1 (Ackley)	202	178	223	220	156	100
F_2 (Griewank)	489	354	524	218	241	100
F_3 (Rastrigin)	424	276	342	316	301	100
F_4 (Schwefel 2.22)	455	265	423	153	265	100
F_5 (Schwefel 2.26)	205	156	154	128	145	100

Table 3 Filter characteristics

Type of filter	LP	HP	BP	BS
Pass-band (normalized) edge frequency	0.45	0.55	–	–
Stop-band (normalized) edge frequency	0.55	0.45	–	–
Lower stop-band (normalized) edge frequency	–	–	0.25	0.35
Lower pass-band (normalized) edge frequency	–	–	0.35	0.25
Upper pass-band (normalized) edge frequency	–	–	0.65	0.85
Upper stop-band (normalized) edge frequency	–	–	0.75	0.75
Transition width	0.1	0.1	0.1	0.1
Pass-band ripple	0.1	0.1	0.1	0.1
Stop-band ripple	0.01	0.01	0.01	0.01

where F(it) represents the objective function value at it iteration by MFO leader; α is set to 0.05.
The position of MFO leader is updated by Powell's method and life span is halved. Due to which, the frequency to update the MFO leader by Powell's method will be doubled.
ELSE
The life span of MFO leader is doubled and the frequency to update the MFO leader by Powell's method will be halved.
ENDIF

Step 8: Check the termination criteria, which is based on maximum number of iterations as:
IF ($it > it^{max}$)
MFO leader position represents the global best solution.
ELSE
GO TO Step 4.
STOP

Table 4 The stop-band attenuation for FIR LP filter

Algorithm	Stop-band attenuation (dB)				Transition width (normalized)	Average execution time (sec)
	Max	Min	Avg	SD		
PSO	34.5903	38.2728	36.57234	0.631557	0.1015	15.76
Chaotic DE	21.4278	29.24362	26.73065	1.806425	0.1250	15.32
ABC	18.4999	21.67092	20.4954	0.779655	0.0937	17.44
GWO	34.0667	40.72424	39.5065	1.122392	0.0937	15.33
MFO	34.4719	37.4579	36.34982	0.731962	0.1015	14.29
DE [5]	–	–	–	–	>0.16	–
DE [5]	–	–	–	–	>0.06	–
DE-PSO [16]	<27	–	–	–	–	–
CSO [28]	33.99	–	–	–	–	–
Proposed	35.139	37.65457	36.98977	0.546765	0.0859	12.40

4 Results and Discussion

In this work, two experiments have been carried out and the MATLAB 8.1 version on Intel Core i5-6440HQ processor, 2.3 GHz with 8 GB RAM has been used. In the first experiment, the proposed technique has been tested on standard benchmark functions. In the second experiment, LP, HssP, BP and BS FIR filters of the order of 20 have been optimally designed. For each algorithm, the population size has been taken as 40 with 500 iterations. The algorithm parameters have been set after a number of trials. To consider the effect of random initialization, thirty trails have been performed for each applied algorithm and the best, worst and average values of objective function have been computed. Further, standard deviation is also tabulated. The parametric statistical t test (two samples, two tails) has been conducted to investigate the significance of the proposed optimization technique.

4.1 Experiment 1: Benchmark Functions

The five unconstrained benchmark functions have been undertaken which are multimodal, continuous/discontinuous in nature. The details regarding these functions are given in Table 1 [12]. The PSO, Chaotic DE, ABC, GWO, MFO and proposed technique have been applied to the standard benchmark functions. The normalized optimum results have been presented in Table 2 and the value in each row 100 represents the minimum value and the remaining values are scaled with respect to the minimum value. The results disclose that the proposed optimization technique is capable of exploring the optimum results for all considered standard benchmark functions. Further, it has also been observed that for Griewank, Schewefel (2.22) and Schewefel (2.26) benchmark functions, GWO technique performs well as compared to PSO, Chaotic DE, ABC and MFO techniques. However, for Ackley and Rastrigin benchmark functions, the MFO technique is able to attain moderate solutions. Hence, it

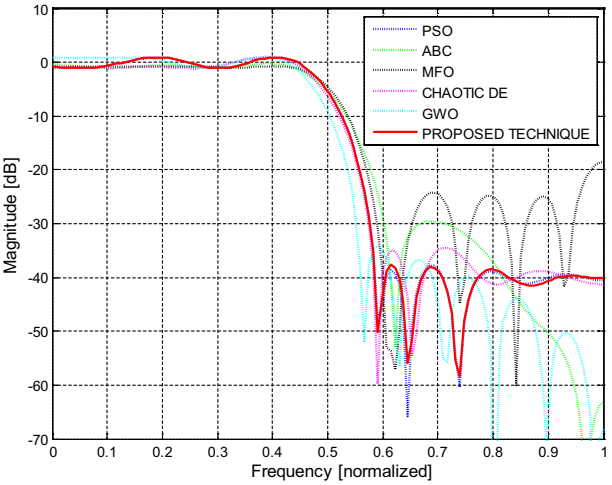

Fig. 1 Magnitude (dB) plot for the FIR LP filter

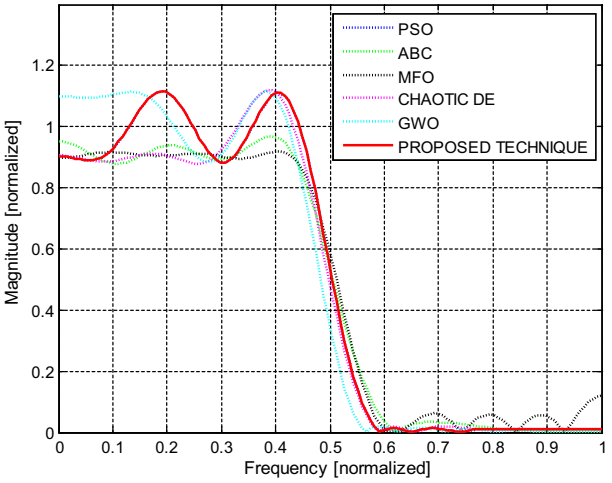

Fig. 2 Magnitude (normalized) plot for the FIR LP filter

is summarized that, the enclosure of PPS method with MFO technique improves the quality of solution.

4.2 Experiment 2: Filter Design

In this research work, the optimum filter coefficients for 20th order LP, HP, BP and BS FIR filters are searched by applying PSO, Chaotic DE, ABC, GWO, MFO and proposed optimization technique. The upper and lower limits of filter coefficients are set to +1 and −1, respectively. The FIR filter parameters have been referred from Saha et al. [28] and are given in Table 3.

Table 5 The stop-band ripple (normalized) for the FIR LP filter

Algorithm	Stop-band ripple (normalized)				*t* Test for average of stop-band ripple	*p* value	Outcome
	Max	Min	Avg	SD			
PSO	0.0186	0.0122	0.014877	0.001104	2.675452	0.009683294	Reject
Chaotic DE	0.0848	0.0345	0.047097	0.010652	16.86597	4.93028E–24	Reject
ABC	0.1189	0.0825	0.09483	0.008711	50.42642	1.33132E–49	Reject
GWO	0.0198	0.0092	0.010687	0.001802	9.394889	2.97732E–13	Reject
MFO	0.0189	0.0134	0.015277	0.001327	3.733801	0.000432031	Reject
DE [5]	>0.09	–	–	–	NA	NA	NA
DE [5]	>0.07	–	–	–	NA	NA	NA
DE-PSO [16]	0.270	–	–	–	NA	NA	NA
CSO [28]	0.02085	–	–	–	NA	NA	NA
Proposed	0.0175	0.0131	0.01417	0.000936	–	–	–

Table 6 The pass-band ripple (normalized) for the FIR LP filter

Algorithm	Pass-band ripple (normalized)			
	Max	Min	Avg	SD
PSO	0.1174	0.0823	0.100713	0.007893
Chaotic DE	0.1942	0.0923	0.124717	0.03157
ABC	0.1662	0.0997	0.128087	0.02384
GWO	0.1544	0.1004	0.136963	0.01678
MFO	0.1517	0.1021	0.12583	0.019049
DE [5]	>0.08	–	–	–
DE [5]	0.040	–	–	–
DE-PSO [16]	0.291	–	–	–
CSO [28]	0.164	–	–	–
Proposed	0.1163	0.0889	0.105157	0.005355

4.2.1 Low-pass Filter Design

The performance parameters, i.e., maximum stop-band attenuation, maximum stop-band ripples and pass-band ripples, of the LP filter designed by the proposed optimization technique have been compared with the results obtained by PSO, Chaotic DE, ABC, GWO and MFO techniques. Further, these are compared with the reported results of the literature, which is obtained by DE [10], DE-PSO [16] and CSO [28] techniques. The maximum, minimum and average stop-band attenuation along with the standard deviation (SD) for various optimization techniques are presented in Table 4. The maximum value of stop-band attenuation obtained by proposed technique is superior by 1.56%, 39.01%, 47.35%, 3.05%, 1,89%, 23.16% and 3.26% for PSO, Chaotic DE, ABC, GWO, MFO, DE-PSO [16] and CSO [28] techniques, respectively. From

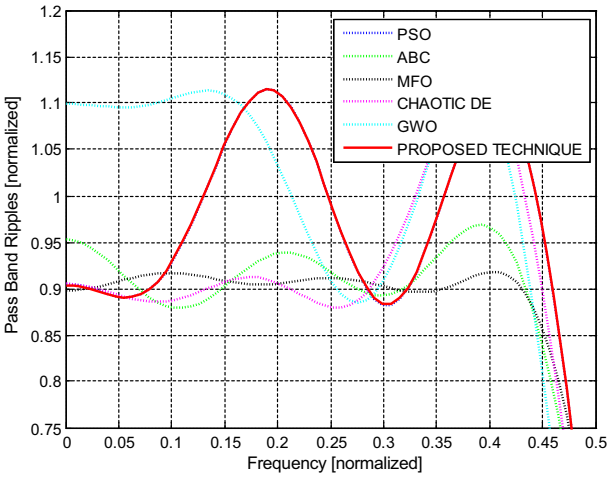

Fig. 3 Normalized pass-band ripple plot for the FIR LP filter

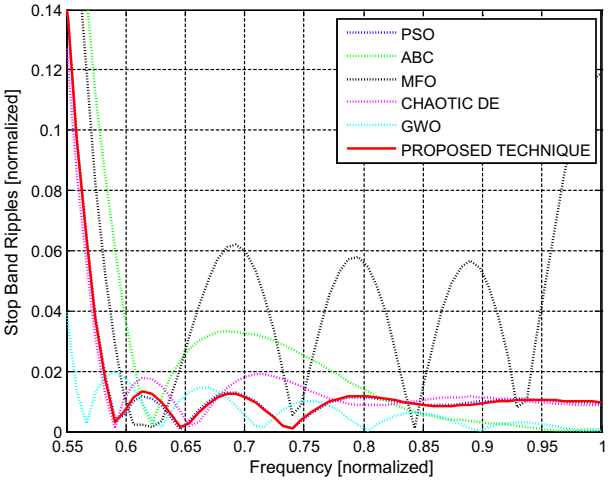

Fig. 4 Normalized stop-band ripple plot for the FIR LP filter

Table 4, it can also be summarized that the proposed optimization technique outperforms its counterparts in terms of maximum, minimum and average values of stop-band attenuation. Further, the standard deviation of the results obtained by proposed optimization technique is minimal, that indicates the proposed optimization technique is capable to achieve better results, repetitively. Figures 1 and 2 illustrate the magnitude response in dB and normalized magnitude response, respectively. The magnitude response of a filter is restricted by normalized transition width, and after analysing the results, it has been observed that proposed technique is able to restrict the transition width within approved limit. However, the transition width reported for PSO, Chaotic DE, MFO and DE [5] techniques violate the prescribed limits.

Table 7 Optimized coefficients of the FIR LP filter ($\times 10^{-02}$)

h(N)	PSO	Chaotic DE	ABC	GWO	MFO	Proposed technique
h(1)	−1.51	0.65	−1.78	1.49	0.76	−1.48
h(2)	−3.07	1.5	2.5	1.49	1.57	−3.06
h(3)	0.33	0.45	0.037394	−2.69	−1.06	0.34
h(4)	5.15	−2.09	−2.3	−4.63	−3.93	5.16
h(5)	1.99	−0.74	−1.22	1.00	0.59	2
h(6)	−4.49	4.54	4.54	6.29	6.75	−4.5
h(7)	0.05	1.52	1	−0.05	0.55	0.05
h(8)	10.69	−9.32	−8.17	8.81	−10.84	10.72
h(9)	1.75	−1.44	−2.01	2.61	−1.96	1.75
h(10)	−31.14	29.17	28.84	33.13	28.87	−31.15
h(11)	−50	46.79	46.88	50.26	47.94	−50

Table 8 The stop-band attenuation for HP FIR filter

Algorithm	Stop-band attenuation (dB)				Transition width (normalized)	Average execsution time (sec)
	Max	Min	Avg	SD		
PSO	31.1377	37.1397	36.40007	1.047207	0.0859	15.89
Chaotic DE	27.0528	38.78604	32.92297	3.564049	0.0937	15.77
ABC	28.9288	37.78821	35.55216	2.271728	0.109	17.43
GWO	32.8795	40.2645	36.62026	3.728704	0.0859	15.39
MFO	29.4230	38.93843	34.94033	3.079899	0.1015	14.82
CSO [28]	33.62	–	–	–	0.0941	–
Proposed	37.0621	40.72424	39.96202	0.652463	0.0937	11.82

Table 9 The stop-band ripple (normalized) for the FIR HP filter

Algorithm	Stop-band ripple (normalized)				*t* Test for average of stop-band ripple	*p* value	Outcome
	Max	Min	Avg	SD			
PSO	0.0277	0.0139	0.015263	0.002419	11.09122	5.81512E–16	Reject
Chaotic DE	0.0444	0.0115	0.024383	0.009216	8.468985	1.00742E–11	Reject
ABC	0.0358	0.0129	0.01734	0.005677	6.934516	3.7755E–09	Reject
GWO	0.0227	0.0097	0.01628	0.008136	4.156145	0.000107921	Reject
MFO	0.0338	0.0113	0.0191	0.007410	6.629291	1.22595E–08	Reject
CSO [28]	0.02085	–	–	–	NA	NA	NA
Proposed	0.0140	0.0092	0.010073	0.000847	–	–	–

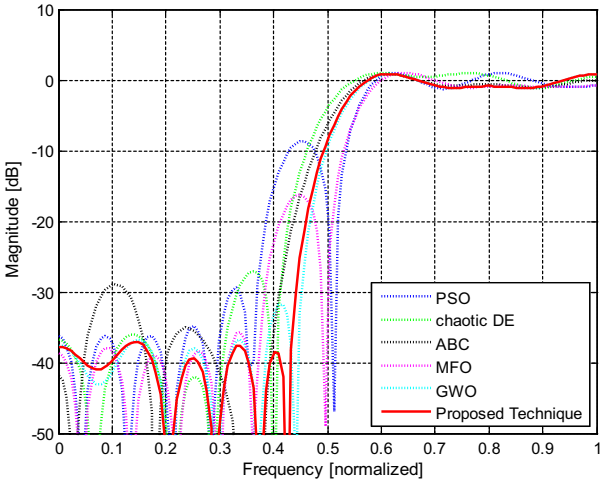

Fig. 5 Magnitude (dB) plot for the FIR HP filter

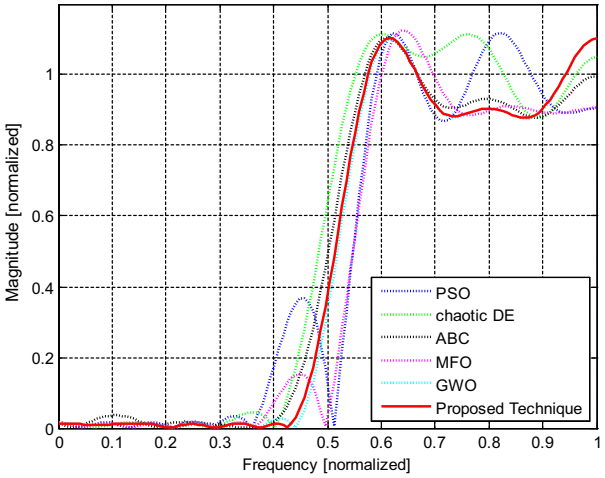

Fig. 6 Magnitude (normalized) plot for the FIR HP filter

In order to compare the computational effort, the PSO, Chaotic DE, ABC, GWO and MFO techniques have been executed thirty times and average execution time of each algorithm has been computed and presented in Table 4. The average execution time required by proposed technique is 12.40 s, while MFO technique needs 14.29 s for it. Hence, it is summarized that integration of MFO with Powell's conjugate direction method improves the exploitation capability of the proposed technique and reduces the computational burden. The statistical values of other two performance parameters, i.e. normalized stop-band ripples and pass-band ripples are presented in Tables 5 and 6, respectively. The maximum value of normalized stop-band ripple achieved by proposed optimization technique is restricted to 0.0175, which is superior as compared

Table 10 The pass-band ripple (normalized) for the FIR HP filter

Algorithm	Pass-band ripple (normalized)			
	Max	Min	Avg	SD
PSO	0.1376	0.1012	0.11147	0.009589
Chaotic DE	0.1227	0.0987	0.10932	0.007499
ABC	0.1199	0.1021	0.107676	0.004923
GWO	0.1242	0.0945	0.11098	0.007829
MFO	0.1350	0.1034	0.113547	0.008655
CSO [28]	0.1320	–	–	–
Proposed	0.1216	0.1045	0.11473	0.005187

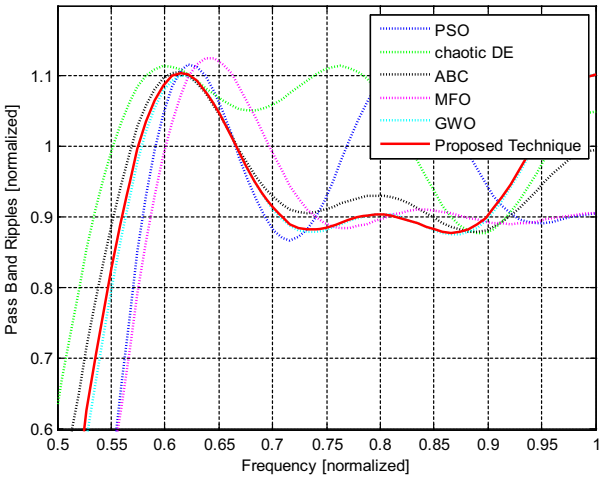

Fig. 7 Normalized pass-band ripple plot for the FIR HP filter

to results obtained by other state of art optimization techniques. In addition to that, the other statistical values, i.e. average value, minimum value of stop-band ripple and SD of proposed technique is better than its counterparts.

The maximum value of normalized pass-band ripple achieved by proposed optimization technique is restricted to 0.1163, which is better than its counterparts except the results reported for DE technique [5]. However, the results of DE [5] technique is inferior as compared to results obtained by proposed technique. The statistical results of pass-band ripple are also compared and it is summarized that performance of proposed technique is better than other compared optimization techniques. Further, the statistical t test has been performed on average value of stop-band ripples with a 95% level of confidence.

It has been found from t test results that p value is less than 0.05, which shows that the proposed technique is significantly better than other optimization techniques. The normalized pass-band and stop-band ripples are presented in Figs. 3 and 4, respectively, and it is demonstrated that proposed optimization technique is able to bottle up the ripples as per the prescribed limits. The optimized LP filter coefficients obtained by

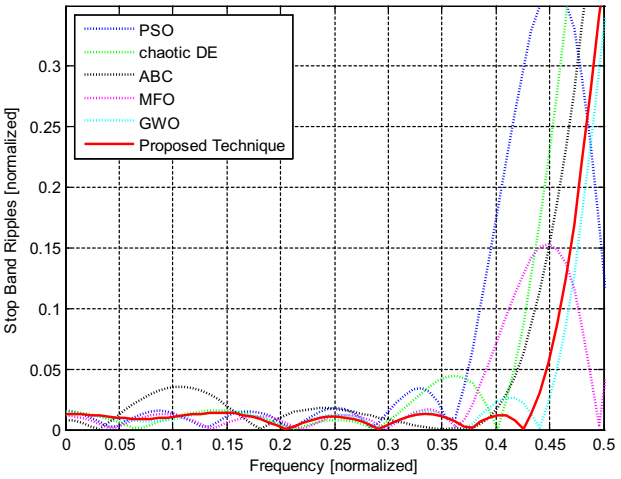

Fig. 8 Normalized stop-band ripple plot for the FIR HP filter

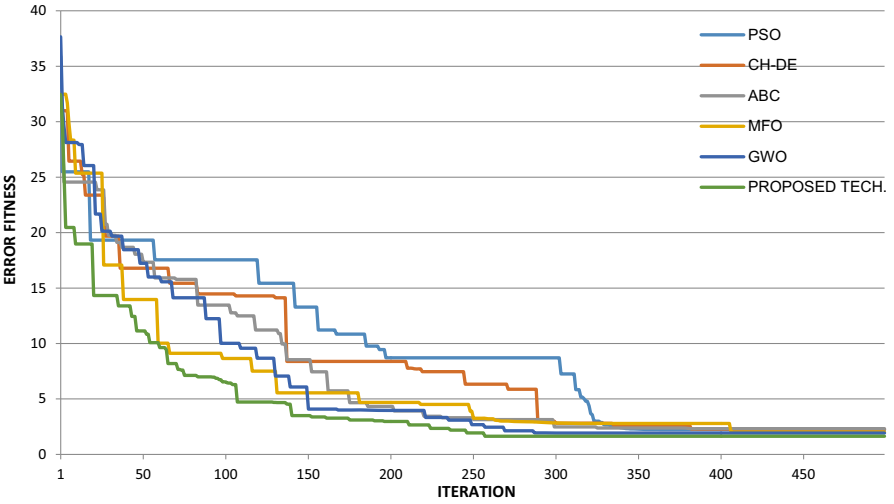

Fig. 9 Convergence characteristics of various optimization techniques for HP filter

PSO, Chaotic DE, ABC, GWO, MFO and proposed optimization technique have been presented in Table 7.

4.2.2 High-Pass Filter Design

The statistical results of stop-band attenuation are given in Table 8 for HP filter. It has been evident from Table 8 that the maximum stop-band attenuation obtained by proposed optimization technique is 37.06 dB, which is considerably better than as compared to PSO, chaotic DE, ABC, GWO, MFO and CSO [28] techniques. The statistical results also confirm the better search ability of proposed optimization tech-

Table 11 Optimized coefficients of the FIR HP filter ($\times 10^{-02}$)

h(N)	PSO	Chaotic DE	ABC	GWO	MFO	Proposed technique
h(1)	2.78	0.78	−1.43	1.87	1.21	1.68
h(2)	−3.16	−2.62	1.58	−2.35	−3.43	−2.31
h(3)	−1.93	2.22	0.19	−1.41	0.98	−1.15
h(4)	5.04	2.28	−3.31	2.87	4.53	2.85
h(5)	−0.14	−0.43	−0.95	2.80	−2.97	2.42
h(6)	−4.84	−5.57	6.55	−7.47	−4.36	−7.44
h(7)	−1.94	0.63	−0.74	0.022	1.18	0.73
h(8)	11.03	12.11	−10.03	9.69	10.79	9.67
h(9)	0.61	−2.94	2	1.01	−3.41	0.45
h(10)	−30	−32.09	29.89	−29.97	−30	−30
h(11)	47.54	52.72	−48.31	46.80	52	47.5

Table 12 The stop-band attenuation for FIR BP filter

Algorithm	Stop-band attenuation (dB)				Transition width (normalized)		Average execution time (sec)
	Max	Min	Avg	SD			
PSO	35.1701	40.72424	38.91029	1.410959	0.0859	0.0937	15.90
Chaotic DE	31.5647	39.01564	36.92573	1.424687	0.1015	0.117	15.28
ABC	23.4482	32.91783	28.3081	2.656215	0.1015	0.117	17.62
GWO	21.7981	37.0156	29.9971	4.72126	0.1015	0.117	15.77
MFO	32.8419	37.20242	35.21568	1.556039	0.0937	0.117	13.98
CSO [28]	34.470	–	–	–	0.1006	0.1006	–
Proposed	36.1814	39.828	37.61488	1.007784	0.0859	0.0859	12.55

nique as compared to other state of art optimization techniques. Another performance parameter 'transition width' is well satisfied by all techniques. In order to judge the computational performance, average computational time has been compared and found that, proposed technique needs less time to search better solution as compared to other compared optimization techniques. The dB plot and normalized magnitude plot for the HP filter realized by various optimization techniques are shown in Figs. 5 and 6, respectively.

The statistical results of other two performance parameters, i.e. stop-band and pass-band ripples are tabulated in Tables 9 and 10, respectively. It has been found from these results that the proposed optimization technique is able to purge the stop-band and pass-band ripples at a better satisfactory level as compared to other compared techniques. The t test results of Table 9, endorse the superiority of the proposed optimization technique as compared to other techniques. The normalized pass-band and stop-band ripples are presented in Figs. 7 and 8, respectively. The convergence characteristics of PSO, Chaotic DE, ABC, GWO, MFO and proposed technique for HP filter are depicted in Fig. 9. It is illustrated from convergence characteristics that proposed

Table 13 The stop-band ripple (normalized) for the FIR BP filter

Algorithm	Stop-band ripple (normalized)				*t* Test for average of stop-band ripple	*p* value	Outcome
	Max	Min	Avg	SD			
PSO	0.0174	0.0092	0.011337	0.001928	4.117378	0.00012293	Reject
Chaotic DE	0.0264	0.0112	0.014247	0.002746	1.911203	0.060924369	Accept
ABC	0.0672	0.0226	0.038423	0.011575	11.85893	3.85692E–17	Reject
GWO	0.0813	0.0141	0.031633	0.017105	5.893522	2.04064E–07	Reject
MFO	0.0228	0.0138	0.017347	0.003187	6.533471	1.77266E–08	Reject
CSO [28]	0.01891	–	–	–	NA	NA	NA
Proposed	0.0155	0.0102	0.013160	0.001471	–	–	–

Table 14 The pass-band ripple (normalized) for the FIR BP filter

Algorithm	Pass-band ripple (normalized)			
	Max	Min	Avg	SD
PSO	0.1999	0.1224	0.15727	0.0249
Chaotic DE	0.1501	0.1123	0.13144	0.00869
ABC	0.1171	0.0226	0.038423	0.011575
GWO	0.2143	0.1021	0.14631	0.03219
MFO	0.1838	0.1427	0.1648	0.0119
CSO [28]	0.163	–	–	–
Proposed	0.1484	0.1256	0.13532	0.00598

Table 15 Optimized coefficients of the FIR BP filter ($\times 10^{-02}$)

h(N)	PSO	Chaotic DE	ABC	GWO	MFO	Proposed technssique
h(1)	−2.27	1.12	−0.29	−0.13	3.52	1.56
h(2)	−1.7	−0.07625	0.21	1.09	−0.08	1.66
h(3)	5.12	−4.19	4.16	3.68	−6.75	−4.93
h(4)	2.68	−0.12	0.83	−2.63	0.12	−2.78
h(5)	−2.56	2.38	−4.01	4.98	3.31	2.8
h(6)	−1.48	0.17	0.019609	2.11	−0.05	1.51
h(7)	−10.39	11.05	−8.92	6.86	10.78	9.61
h(8)	−0.2	0.64	−0.88	−0.20	−0.08	0.39
h(9)	27.44	−30.77	31.79	−28.93	−28.78	−27.74
h(10)	0.64	−0.08998	0.52	−0.06	0.06	−0.71
h(11)	−35.79	40.22	−42.72	40.61	37.11	36.38

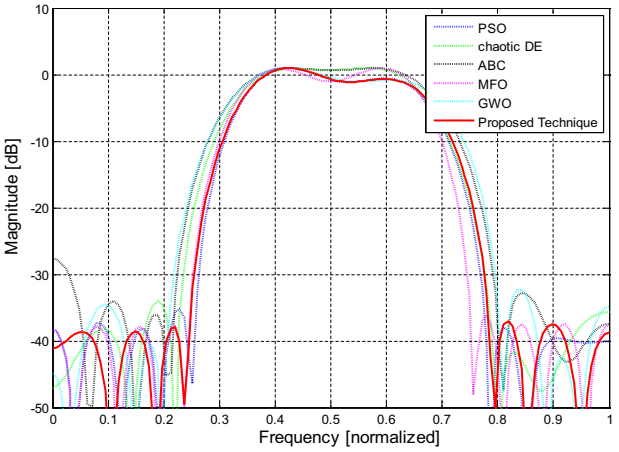

Fig. 10 Magnitude (dB) plot for the FIR BP filter

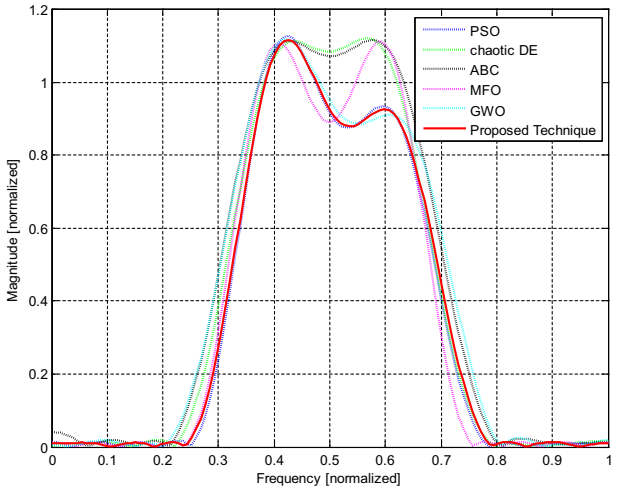

Fig. 11 Magnitude (Normalized) plot for the FIR BP filter

technique needs less iteration as compared to other compared techniques to search the global best solution. The optimized coefficients of HP filter, obtained by PSO, Chaotic DE, ABC, GWO, MFO and proposed optimization technique are presented in Table 11.

4.2.3 Band-pass Filter Design

For band-pass filter design, the result of proposed technique is compared with PSO, chaotic DE, ABC, GWO, MFO and CSO [28] techniques and are presented in Table 12. The maximum stop-band attenuation obtained by proposed optimization technique for BP filter is 36.18 dB, which is 2.79%, 12.75%, 35.19% 39.75%, 9.22% and 4.73%

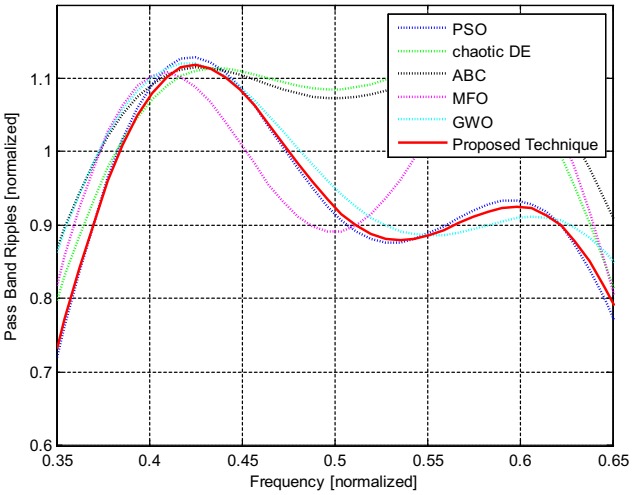

Fig. 12 Normalized pass-band ripple plot for the FIR BP filter

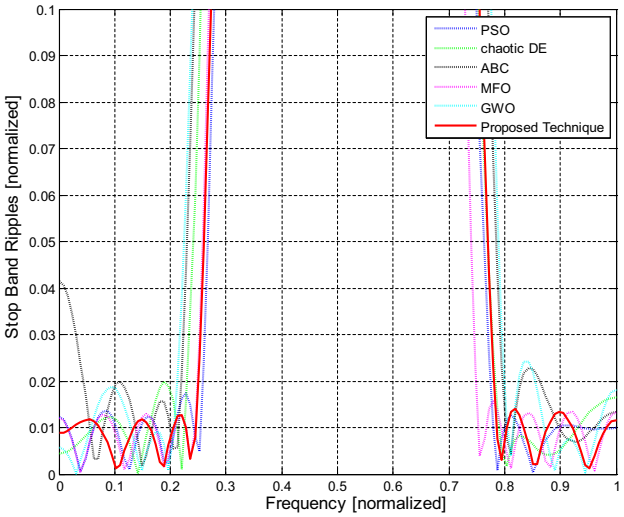

Fig. 13 Normalized stop-band ripple plot for the FIR BP filter

better as compared to results obtained by PSO, Chaotic DE, ABC, GWO, MFO and CSO [28] techniques, respectively. It has been observed from Table 12 that proposed optimization technique is able to maintain the transition widths within the restricted limits, while other optimization techniques violates the restricted limits by small margins. Further, the standard deviation of thirty trials is 1.007, which is minimum that indicates the proposed optimization technique produces superior results, repetitively. The proposed optimization technique needs 12.55 s to reach its global best solution, which is better as compared to MFO and other optimization techniques. Hence, it can be summarized that integration of MFO with PPS in a logical manner improves

the exploitation capability of the search algorithm. The dB and normalized plot for the BP filter are illustrated in Figs. 10 and 11, respectively. The statistical values of stop-band and pass-band ripple are presented in Tables 13 and 14, respectively. It has been observed from these results that proposed technique is able to achieve superior results in terms of maximum, minimum, average value and SD. The t test has been performed at the 95% level of confidence on the average value of stop-band ripples statistically. It has been found that proposed optimization technique is significantly better than its counterparts. However, for stop-band ripples, the chaotic DE technique performs at par with proposed technique. Figures 12 and 13 represent the normalized pass-band and stop-band ripples of BP filter by various optimization techniques. The optimal coefficients of BP filter are presented in Table 15.

4.2.4 Band-stop Filter Design

For band-stop filter, the results are compared with PSO, Chaotic DE, ABC, GWO, MFO, CSO [28], PM [8], RGA [8], CLPSO [8] and CRPSO [8] techniques and are presented in Table 16. The maximum stop-band attenuation obtained by proposed optimization technique is 35.0251 dB, which is better than other compared techniques. The statistical results validate the dominance of proposed optimization technique as compared to other techniques in terms of attenuation. The normalized transition width and average execution time are also represented in Table 16. The average execution time taken by PSO, Chaotic DE, ABC, GWO, MFO and proposed optimization technique on similar operational environment is 15.25 s, 14.98 s, 17.66 s, 15.81 s, 13.98 s, 12.04 s, respectively. From these results, it is evident that proposed optimization technique needs less computational efforts among all these techniques. Tables 17 and 18 represent the maximum, minimum and average values of pass-band and stop-band ripples. It has been noticed that the proposed optimization technique is capable to achieve all the desired attributes of band-pass filter consistently.

Further, the t test also verifies the credibility of the proposed optimization technique at 95% level of confidence. However, for stop-band ripples, the GWO technique performs at par with proposed technique statistically. For band-stop filter, Figs. 14, 15, 16 and 17 show the magnitude response, pass-band and stop-band ripples using PSO, Chaotic DE, ABC, GWO and MFO techniques. The optimal coefficients of band-stop filter obtained by proposed optimization technique are presented in Table 19.

5 Conclusions

In this work, an optimal FIR filter has been designed using PSO, Chaotic DE, ABC, GWO, MFO and proposed optimization techniques. The proposed optimization technique combines the excellent exploration capability of MFO technique and the superior exploitation property of the PPS method. During the search process, the adaptive life span controls the switching of MFO leader from MFO technique to PPS method, which helps to explore the search area with adequate computational efforts. The proposed optimization technique has been tested on five benchmark functions and subsequently, it is applied for an optimum design of LP, HP, BP and BS FIR filters. The results reveal

Table 16 The stop-band attenuation for FIR BS filter

Algorithm	Stop-band attenuation (dB)				Transition width (normalized)		Average execution time (sec)
	Max	Min	Avg	SD			
PSO	25.5562	39.09354	32.57363	3.789917	0.0937	0.1015	15.25
Chaotic DE	23.7110	38.2019	30.2562	3.602255	0.1015	0.117	14.98
ABC	25.0170	38.93843	31.85545	3.627802	0.109	0.0859	17.66
GWO	33.8074	38.2728	36.5077	1.33030	0.1015	0.0859	15.81
MFO	30.8326	38.2019	35.49902	1.912967	0.0937	0.0937	13.98
CSO [28]	32.11	–	–	–	0.1034	0.1034	–
PM [8]	14.18	–	14.18	0.0126	–	–	–
RGA [8]	14.92	–	15.61	0.9059	–	–	–
CLPSO [8]	16.51	–	16.55	0.0236	–	–	–
CRPSO [8]	17.57	–	18.03	0.5406	–	–	–
Proposed	35.0251	37.4579	36.62459	0.56547	0.1015	0.0937	12.04

Table 17 The stop-band ripple (normalized) for the FIR BS filter

Algorithm	Stop-band ripple (normalized)				*t* Test for average of stop-band ripple	*P* value	Outcome
	Max	Min	Avg	SD			
PSO	0.0527	0.0111	0.02563	0.010314	5.735665	3.70204E–07	Reject
Chaotic DE	0.0652	0.0123	0.033143	0.012515	8.011743	5.85335E–11	Reject
ABC	0.0561	0.0113	0.02763	0.01069	6.556058	1.62516E–08	Reject
GWO	0.0128	0.0122	0.015127	0.002468	0.715036	0.477455052	Accept
MFO	0.0287	0.0123	0.017213	0.004157	3.11899	0.002825003	Reject
CSO [28]	0.02479	–	–	–	NA	NA	NA
PM [8]	0.195	–	–	–	NA	NA	NA
RGA [8]	0.179	–	–	–	NA	NA	NA
CLPSO [8]	0.149	–	–	–	NA	NA	NA
CRPSO [8]	0.132	–	–	–	NA	NA	NA
Proposed	0.0177	0.0134	0.01478	0.000987	–	–	–

that it has been able to achieve the better solution as compared to results obtained by PSO, Chaotic DE, ABC, GWO and MFO techniques for benchmark functions. For filter design problem, the proposed optimization technique is able to achieve maximum stop-band attenuation, the lowest stop-band and pass-band ripples with adequate transition width. Further, the obtained results have been compared by results reported for other state of art optimization techniques, *i.e.*, DE, DE-PSO, CSO. From the reported results, CSO shows better quality results. Hence, the results of proposed technique are compared with CSO technique in a comprehensive manner. For LP filter, the

Table 18 The pass-band ripple (normalized) for the FIR BS filter

Algorithm	Pass-band ripple (normalized)			
	Max	Min	Avg	SD
PSO	0.1626	0.1123	0.144693	0.015356
Chaotic DE	0.1444	0.1131	0.126263	0.010778
ABC	0.2036	0.1602	0.187727	0.009799
GWO	0.1211	0.0197	0.11100	0.017921
MFO	0.2309	0.1134	0.185913	0.042199
CSO [28]	0.144	–	–	–
PM [8]	0.196	–	–	–
RGA [8]	0.12	–	–	–
CLPSO [8]	0.07	–	–	–
CRPSO [8]	0.095	–	–	–
Proposed	0.1295	0.1121	0.12095	0.00545

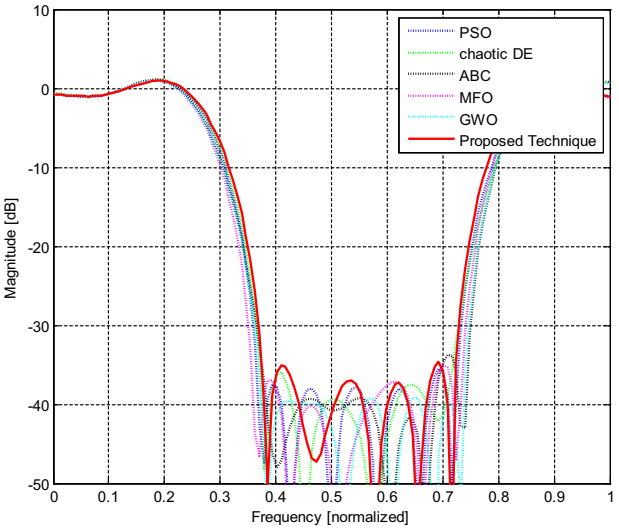

Fig. 14 Magnitude (dB) plot for the FIR BS filter

maximum stop-band attenuation, maximum stop-band ripple, maximum pass-band ripple and transition width reported for CSO technique are 33.99 dB, 0.01998, 0.164 and 0.0946, respectively, while, the proposed technique is able to achieve better corresponding performance parameters for LP filter, i.e. 35.139, 0.0175, 0.1163 and 0.0857. The proposed technique is able to improve the maximum stop-band attenuation for HP, BP, BS filters by 10.23%, 4.96% and 9.07%, respectively, as compared to results reported for CSO technique. The proposed technique shows its superiority in other two performance parameters 'maximum stop-band ripple' and 'maximum pass-band ripple' as compared to CSO technique results. The maximum stop-band ripple is improved by 32.85%, 18.03%, 28.60%, and maximum pass-band ripple is improved

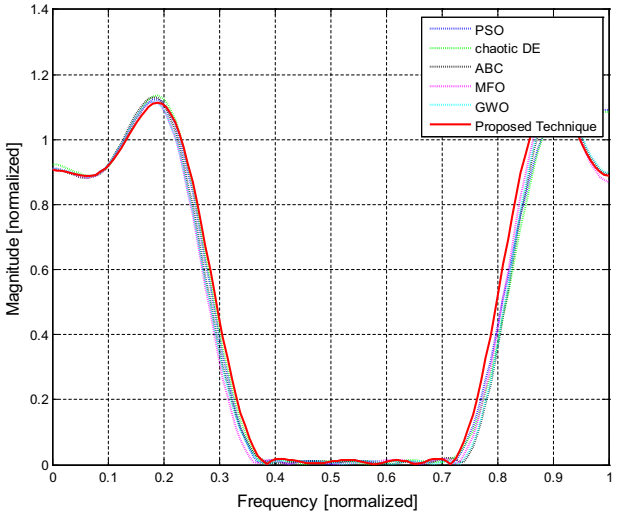

Fig. 15 Magnitude (normalized) plot for the FIR BS filter

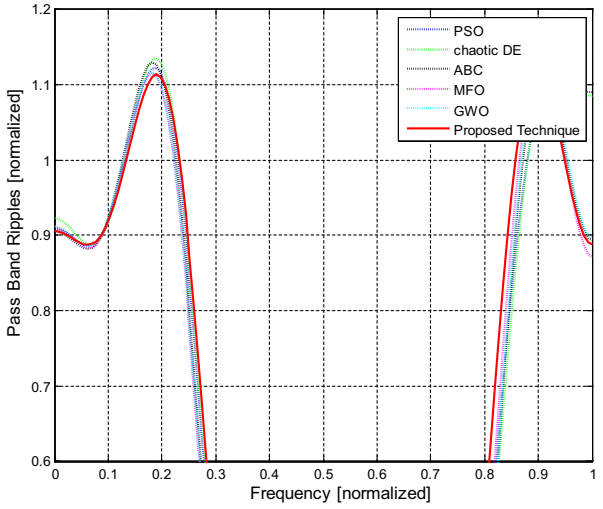

Fig. 16 Normalized pass-band ripple plot for the FIR BS filter

by 7.87%, 8.95% 10.06% for HP, BP and BS filters, respectively. The proposed technique maintains another performance parameter 'transition width' within the specified limits. Further, the robustness of the proposed optimization technique is investigated by applying statistical t test and performance is found satisfactory. Finally, it has been concluded that the proposed optimization technique is more robust, computationally efficient and a better global optimizer .

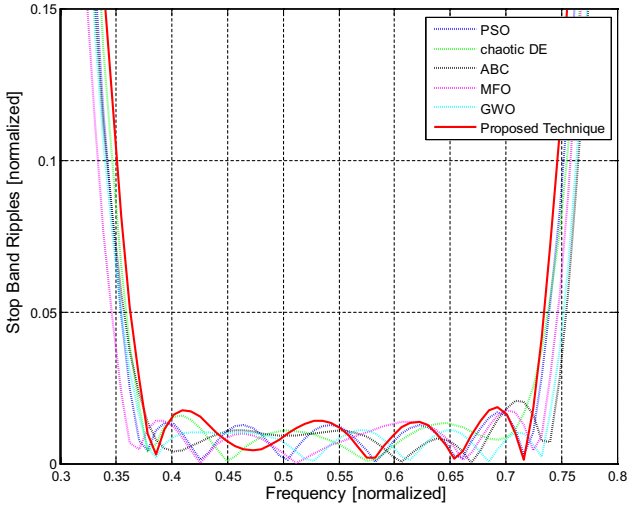

Fig. 17 Normalized stop-band ripple plot for the FIR BS filter

Table 19 Optimized coefficients of the FIR BS filter ($\times 10^{-02}$)

h(N)	PSO	Chaotic DE	ABC	GWO	MFO	Proposed technique
h(1)	0.75	−2.04	2.81	2.91	2.69	0.23
h(2)	3.67	−0.56	−0.42	−0.65	−0.14	3.99
h(3)	−0.18	−4.46	5.07	4.99	5.26	−1.21
h(4)	1.94	2.22	−4.2	−4.12	−4.82	4.09
h(5)	−5.5	3.28	−2.51	−2.27	−2.05	−6.83
h(6)	−8.04	4.99	−5.61	−5.65	−6.09	−6.12
h(7)	0.69	10.73	−9.54	−9.40	−8.75	−1.46
h(8)	−7.69	−13.21	13.12	13.42	13.36	−7.18
h(9)	29.72	1.04	−0.36	−0.27	−0.21	29.24
h(10)	5.61	−43.63	42.11	42.21	42.26	5.69
h(11)	48.99	−9.06	9.74	8.85	8.18	49.74

Data Availability The input dataset is publicly available and detailed output data are given in the manuscript.

Compliance with Ethical Standards

Conflict of interest The author declare that they have no conflict of interest.

Ethical Approval This article does not contain any studies with human participants or animals performed by any of the authors.

References

1. A. Aggarwal, T.K. Rawat, D.K. Upadhyay, Design of optimal digital FIR filters using evolutionary and swarm optimization techniques. Int. J. Electron. Commun. **70**(4), 373–385 (2016)
2. A. Aggarwal, T.K. Rawat, M. Kumar, D.K. Upadhyay, Optimal design of FIR high pass filter based on L_1 error approximation using real coded genetic algorithm. Eng. Sci. Technol. Int. J. **18**(4), 594–602 (2015)
3. M.A.E. Aziz, A.A. Ewees, A.E. Hassanien, Whale optimization algorithm and moth-flame optimization for multilevel thresholding image segmentation. Expert Syst. Appl. **83**, 242–256 (2017)
4. A. Das, D. Mandal, S.P. Ghoshal, R. Kar, Concentric circular antenna array synthesis for side lobe suppression using moth flame optimization. Int. J. Electron. Commun. **86**, 177–184 (2018)
5. J. Dash, B. Dam, R. Swain, Optimal design of linear phase multi-band stop filters using improved cuckoo search particle swarm optimization. Appl. Soft Comput. **52**, 435–445 (2017)
6. A.A. Elsakaan, R.A. EI-Sehiemy, S.S. Kaddah, M.I. Elsaid, An enhanced moth-flame optimizer for solving non-smooth economic dispatch problems with emissions. Energy **157**, 1063–1078 (2018)
7. M. Harman, P. McMinn, A theoretical and empirical study of search-based testing: local, global, and hybrid search. IEEE Trans. Softw. Eng. **36**(2), 226–247 (2010)
8. R. Kar, D. Mandal, S. Mondal, S.P. Ghoshal, Craziness based particle swarm optimization algorithm for FIR band stop filter design. Swarm Evol. Comput. **7**, 58–64 (2012)
9. D. Karaboga, B. Basturk, A powerful and efficient algorithm for numerical function optimization: artificial bee colony (ABC) algorithm. J. Global Optim. **39**, 459–471 (2007)
10. N. Karaboga, B. Cetinkaya, Design of digital FIR filters using differential evolution algorithm. Circuits Syst. Signal Process. **25**(5), 649–660 (2006)
11. J. Kennedy, R. Eberhart, Particle swarm optimization. In: Proceedings of the international conference neural network, Perth, WA, Australia (1995)
12. S. Khalilpourazari, S. Khalilpourazary, An efficient hybrid algorithm based on water cycle and moth-flame optimization algorithms for solving numerical and constrained engineering optimization problems. Soft Comput. **23**, 1699–1722 (2019)
13. C. Li, S. Li, Y. Liu, A least squares support vector machine model optimized by moth-flame optimization algorithm for annual power load forecasting. Appl. Intell. **45**, 1166–1178 (2016)
14. Z. Li, Y. Zhou, S. Zhang, J. Song, Lévy-flight moth-flame algorithm for function optimization and engineering design problems. Math. Problems Eng. (2019). https://doi.org/10.1155/2016/1423930
15. L. Litwin, FIR and IIR digital filters. IEEE Potentials **19**(4), 28–31 (2000)
16. B. Luitel, G.K. Venayagamoorthy, Differential evolution particle swarm optimization for digital filter design. In: IEEE congress on evolutionary computation, pp 3954–3961 (2008)
17. J.H. McClellan, T.W. Parks, L.R. Rabiner, A computer program for designing optimum FIR linear phase digital filters. IEEE Trans. Audio Electroacoust. **21**(6), 506–526 (1973)
18. R.N.S. Mei, M.H. Sulaiman, Z. Mustaffa, H. Daniyal, Optimal reactive power dispatch solution by loss minimization using moth-flame optimization technique. Appl. Soft Comput. **59**, 210–222 (2017)
19. S. Mirjalili, Moth-flame optimization algorithm: a novel nature-inspired heuristic paradigm. Know. Based Syst. **89**, 228–249 (2015)
20. S. Mirjalili, Grey wolf optimizer. Adv. Eng. Softw. **69**, 46–61 (2014)
21. A.A.A. Mohamed, Y.S. Mohamed, A.A.M. EI-Gaafary, A.M. Hemeida, Optimal power flow using moth swarm optimization. Elect. Power Syst. Res. **142**, 190–206 (2017)
22. N. Narang, J.S. Dhillon, D.P. Kothari, Multiobjective fixed head hydrothermal scheduling using integrated predator-prey optimization and powell search method. Energy **47**(1), 237–252 (2012)
23. N. Narang, E. Sharma, J.S. Dhillon, Combined heat and power economic dispatch using integrated civilized swarm optimization and Powell's pattern search method. Appl. Soft Comput. **52**, 190–202 (2017)
24. H.A. Oliveira, A. Petraglia, M.R. Petraglia, Frequency domain FIR filter design using fuzzy adaptive simulated annealing. Circuits Syst. Signal Process. **28**, 899–911 (2009)
25. T.W. Parks, J.H. McCellan, Chebyshev approximation for non recursive digital filters with linear phase. IEEE Trans. Circuit Theory **19**(2), 189–194 (1972)
26. L.R. Rabiner, Approximate design relationship for low-pass FIR digital filters with linear phase. IEEE Trans. Audio Electroacoust **21**(5), 456–460 (1973)

27. K.S. Reddy, L.K. Panwar, B.K. Panigrahi, R. Kumar, Solution to unit commitment in power system operation planning using binary coded modified moth flame optimization algorithm (BMMFOA): a flame selection based computational technique. J. Comput. Sci. **25**, 298–317 (2018)
28. S.K. Saha, S.P. Ghoshal, R. Kar, D. Mandal, Cat swarm optimization algorithm for optimal linear phase FIR filter design. ISA Trans. **52**(6), 781–794 (2013)
29. C.L. Santos, V.C. Mariani, Combining of chaotic differential evolution and quadratic programming for economic dispatch optimization with valve-point effect. IEEE Trans. Power Syst. **21**(2), 989–996 (2006)
30. S.K. Sarangi, R. Panda, P.K. Das, A. Abraham, Design of optimal high pass and band stop FIR filters using adaptive Cuckoo search algorithm. Eng. Appl. Artif. Intell. **70**, 67–80 (2018)
31. P. Singh, S. Prakash, Optical network unit placement in fiber-wireless (FiWi) access network by Moth-Flame optimization algorithm. Opt. Fiber Technol. **36**, 403–411 (2017)
32. S.R. Singiresu, *Engineering Optimization*, 4th edn. (Wiley, Hoboken, 2013).
33. G.G. Wang, Moth search algorithm: a bio-inspired metaheuristic algorithm for global optimization problems. Memetic Comput. **10**(2), 151–164 (2018)
34. M. Wang, H. Chen, B. Yang, X. Zhao, L. Hu, Z. Cai, H. Huamg, C. Tong, Toward an optimal kernel extreme learning machine using a chaotic moth-flame optimization strategy with applications in medical diagnoses. Neurocomputers **267**, 69–84 (2017)
35. W. Xia, S. Xu, J. Lu, Z. Zhang, Y. Chu, Reliable filter design for discrete-time neural networks with Markovian jumping parameters and time-varying delay. J. Franklin Inst. **357**, 2892–2915 (2020)
36. W. Xia, W.X. Zheng, S. Xu, Event-triggered filter design for Markovian jump delay systems with nonlinear perturbation using quantized measurement. Int. J. Robust Nonlinear Control. **29**, 4644–4664 (2019)
37. W. Xia, W.X. Zheng, S. Xu, Extended dissipativity analysis of digital filters with time delay and Markovian jumping parameters, signal processing. Signal Process. **152**, 247–254 (2018)
38. Y. Xu, H. Chen, J. Luo, Q. Zhang, S. Jiao, X. Zhang, Enhanced Moth-flame optimizer with mutation strategy for global optimization. Inf. Sci. **492**, 181–203 (2019)
39. L. Zhang, K. Mistry, S.C. Neoh, C.P. Lim, Intelligent facial emotion recognition using moth-firefly optimization. Know. Based Syst. **111**, 248–267 (2016)